ROBOTICS TODAY

ROBOTICS TODAY focuses on the technology, equipment and applications related to the automated assembly and robotics industries. Feature articles include updates on the latest manufacturing research, tutorials on a particular manufacturing technology and field reports on installed manufacturing technologies, all from a technical perspective. Each issue also includes additional brief articles, product announcements and event listings.

AUTHOR GUIDE

SUBSCRIBE

4th Quarter 2005 Volume 18 No. 4

Content Online

FOURTH QUARTER 2005 **www.sme.org/ama** VOL. 18, NO. 4

ROBOTICS TODAY

Nanorobotics Control Design: A Practical Approach Tutorial

A. Cavalcanti, Center for Automation in Nanobiotech (Sao Paulo SP Brazil);
R.A. Freitas Jr., Institute for Molecular Manufacturing (Palo Alto, Calif.);
and **L.C. Kretly, Unicamp** (Campinas SP Brazil)

Following the first steps toward molecular manufacturing in the 1980s and 1990s with nanoscale building blocks, more complex challenges are now being faced in achieving the next generation of nanotechnology advances, such as with building bionanoelectronics and molecular machines. This article presents the simulation

of mobile multi-robot teams operating at atomic scales to perform biomolecular assembly manipulation for nanomedicine [26]. In such a virtual nanoworld, the teams must cooperate with each other to achieve a productive result in assembling biomolecules into larger biomolecules. The assembled biomolecules must be sequentially delivered into a set of predefined organ inlets, and the nanorobot teams must also keep the nutritional levels of the larger organism under control [9,10]. In the emerging era of biomolecular engineering, the development of methodologies that help focus experimental investigations enabling nanoassembly automation is meaningful. The motivation for such a study is the fact that new approaches for a better comprehension and visualization of nanoworlds aspects can have a great impact on effective design and on the future development of nanotechnology.

One important challenge that has become evident as a vital problem in nanotechnology industrial applications is the automation of atomic-scale manipulation. The starting point of nanotechnology to achieve the main goal of building systems at the nanoscale is the development of control automation for molecular machine systems. Such systems are expected to enable the massively parallel manufacture of nanodevice building blocks. Governments all around the world are directing significant resources toward the fast development of nanotechnology [71,82]. In Germany, the Federal Ministry of Education and Research has announced 50 million Euros to be invested in the years 2002-2006 in research and development on nanotechnology [67]. The U.S. National Science Foundation has launched a program in “Scientific Visualization” [61] in part to harness supercomputers in picturing the nanoworld. A $1 trillion market consisting of devices and systems with some kind of embedded nanotechnology is projected by 2015 [17,59]. More specifically, the firm DisplaySearch predicts rapid market growth from $84 million today to $1.6 billion in 2007 [60]. The miniaturization importance for a broad core of different devices is well known [42], and a first series of commercial nanoproducts has been announced as foreseeable by 2007 [28]. To reach the goal of building organic electronics, firms are forming collaborations and alliances that bring together new nanoproducts through the joint efforts of companies such as IBM, Motorola, Philips Electronics, Xerox/PARC, Hewlett-Packard, Dow Chemical, Bell Laboratories and Intel Corp., among others [28,60]. For such goals, new methodologies and theories to explore the nanoworld are the key to the technology [15].

Building patterns and manipulating atoms with the use of SPMs as in atomic force microscopy (AFM) and scanning tunneling microscopy (STM) has been demonstrated with satisfactory success as a promising approach for the construction of nanoelectromechanical systems (NEMS) with 3-D precision at 0.01 nm resolution [69]. However, such manual manipulations require much time, and even for a repetitive task these manipulations tend to produce imprecise work when performed manually for a large number of molecules. Practical approaches for nano planning systems have been presented as a first step toward automating assembly tasks in nanorobotics, as, for example, in 2-D positional assembly automation [50]. We can expect the first artificial biological nanorobots, a possibility extensively reviewed elsewhere [20,21,23], to become available in five years or less [49]. More complex nanorobots will be manufactured using diamondoid or other similarly rigid materials awaiting primarily our ability to perform positional mechanosynthesis, and work leading in this direction has progressed recently [19,22,56,63,64]. Initial uses of nanorobots in health care are likely to emerge within the next 10 years [26,68,79] with potentially broad biomedical applications [20,26,54,55].

The use of artificial intelligence as the appropriate means to enable some aspects of intelligent behavior in the control of nanorobots during molecular manufacturing automation has been discussed in the nano community [79]. The use of concepts derived from collective robotics and behavior control was investigated for nanomedicine dealing with a common goal to destroy malignant tissues in the

human body [47]. More recent work is progressing toward the development of a nanorobotics autonomous system capable of performing 200,000 accurate measurements per second at atomic scale [51]. An Intel prototype 90 nm process facility has already produced a fully functional 52 Mb SRAM with transistor gate lengths of 50 nm and SRAM cell sizes of just 1 μm^2, or roughly half the cell size of today's most advanced SRAMs [28]. This downscaling will continue, according to the Semiconductor Industry Association's roadmap. By 2016, high-performance ICs will contain more than 8.8 billion transistors in a 280 mm^2 area—more than 25 times as many as on today's chips built with 130 nm feature sizes [28].

A useful starting point for achieving the main goal of building nanoscale devices is the development of generalized automation control for molecular machine systems, which could enable a manufacturing schedule for positional nanoassembly manipulation. In this article, a more specialized scheduling problem with a focus on nanomedicine is considered, for example, describing in a detailed fashion the nanorobot control design and the surrounding virtual workspace modelling that is required for the main kinematics aspects of a physically based nanoworld simulation. Here, the biomolecular assembly manipulation is automatically performed by smart agents, which are given the task of improving the nutritional state of an organism via the injection of appropriate assembled substances into pre-established delivery points in a complex 3-D environment.

The use of smart agents concepts could be found in distinct kinds of application. Intelligent search engines for the Internet [65], security systems [36], anti-virus [62] and anti-spam [16] systems, simulation of artificial life [6] and so on, to quote a few. We could define an agent as an entity able to show predefined capabilities in interacting with events through a specificset of programmed actions [43], using several tools for such aim. Among other tools for agent decision system, in the literature artificial intelligence could be seen[79], fuzzy logic [53], neural networks [16], evolutionary techniques [29], among others. There are biomolecular assemblers that are not defined as nanorobots. They could be natural assemblers [26] as microorganisms, bacterias or artificial assemblers (molecular self-assembly [70]), cellular automata [5] or even a nanorobot. In our work, we have the concept of smart agents applied for the task of assembling biomolecular structures. As we have observed the diverse uses of agents, an agent could be or not be an assembler. For our application, we have smart agents working as assemblers, embodied in the shape of a nanorobot.

Enabling Nanorobots for Nanomedicine

In future decades, the principal focus in medicine will shift from medical science to medical engineering, where the design of medically active microscopic machines will be the consequent result of techniques provided from human molecular structural knowledge gained in the 20th and early 21st centuries [26]. For the feasibility of such achievements in nanomedicine, two primary capabilities for fabrication must be fulfilled: fabrication and assembly of nanoscale parts. Through the use of different approaches, such as biotechnology, supramolecular chemistry, and scanning probes, both capabilities had been demonstrated to a limited degree as early as 1998 [26]. Despite quantum effects that impart a relative uncertainty to electron positions, the quantum probability function of electrons in atoms tends to drop off exponentially with distance outside the atom. Even in most liquids at their boiling points, each molecule is free to move only ~0.07 nm from its average position [26]. Developments in the field of biomolecular computing [1] have demonstrated positively the feasibility of processing logic tasks by bio-computers [33], a promising first step toward building future nanoprocessors with increasing complexity. There has been progress in building biosensors [76] and nanokinetic devices [2,75], which also may be required to enable nanorobotic operations and locomotion. Classical objections related to the feasibility of nanotechnology, such as quantum mechanics, thermal motions and friction, have been considered and resolved, and discussions of techniques for

manufacturing nanodevices are appearing in the literature with increasing frequency [35].

Proposed Approach

Assemblers are molecular machine systems that could be described as systems capable of performing molecular manufacturing at the atomic scale [10]. The collective nanorobotics approach presented here is one possible method to perform a massively-parallel positional nanoassembly manipulation. In the described workspace representing a simplification of the human body, the multi-nanorobot teams perform a pre-established set of tasks building nutrient molecules, crudely analogous to the work done by a ribosome, which is a natural assembler.

Nanorobots monitoring nutrient concentrations in a three-dimensional workspace is a possible application of nanorobots in medicine, among other biomedical problems. One interesting nanorobot application is to assist inflammatory cells (or white cells) leaving blood vessels to repair injured tissues [8]. Also the nanorobot could be used to process specific chemical reactions in the human body as ancillary devices for injured organs [10]. Nanorobots equipped with nanosensors could be developed to detect glucose demand in diabetes patients [40]. Nanorobots could also be applied in chemotherapy to combat cancer through superior chemical dosage administration [45], and a similar approach could be taken to enable nanorobots to deliver anti-HIV drugs [55]. Such drug-delivery nanorobots have been termed “pharmacytes” by Freitas [26].

Three well-known design approaches for nano-manipulation in liquid and air environments [15] include the telescoping robotic arm, the Stewart platform and the five-strut crank model. For this experiment, a robotic arm with nano-manipulation in a liquid environment was chosen the most suitable for an in-vivo nanomedical application. It is also well-known that computation is relatively cheap for macroscale robotic actuators, while arm motion is relatively cheap for nanoscale robotic actuators [15,26]. Thus the moment-by-moment computer control of arm trajectories is the appropriate paradigm for macroscale robots, but not for nanoscale robots. For nanoscale robots, the appropriate manipulator control paradigm is often trajectory trial and error, also known as sensor-based motion control [41].

Techniques to enable rapid design while incorporating complex aspects of physical principles used for production of final 3-D prototypes have been progressing rapidly. Virtual reality techniques are currently being explored successfully in nanoscience and nanotechnology research to provide researchers with an intuitive way to interact with materials and devices at the nanoscale [48]. Guthold [31] tried to provide a virtual-environment interface to scanning probe microscopes (SPMs), giving a virtual telepresence on the surface but downscaled by a factor of about a million to one. The introduction of direct human-SPM interaction creates not only enhanced measurement capability (for instance, special transducers can provide a sense of touch to the nanomanipulator), but also presages a more interactive technology that will enable easy nanofabrication and/or repair of nanostructures. A 3-D bio-nanomanipulation system integrated with a real-time virtual reality simulator has been proposed [27]. Nanoscale object manipulation systems have been applied with the use of computer graphics for teleoperation, where the requirements for such systems have been clearly established [74].

The authors used physically based simulation [3] to consider kinematics and frictional aspects specifically required for rigid body motion with hydrodynamics at low Reynolds number for molecular assembly manipulation.

Virtual Environment

The nanorobot lives in a world of viscosity, where friction, adhesion and viscous forces are paramount, and the gravitational force here is relatively negligible [15,26]. In this world, a very low Reynolds number (*Re*) is assumed for the kinetic calculations [66], where the fluid mechanics in small structures can usually be described by the classical continuum of Eq. (15). The ratio of inertial to viscous forces is determined by as expressed in Eq. (1):

$$Re = \rho VL / \eta \qquad (1)$$

where η is the absolute viscosity of the fluid, V is the velocity, ρ is the fluid density and L is a characteristic dimension. *Re* indicates whether the flow will be laminar or turbulent around an object of a given shape at a given flow velocity. The purpose of Eq. (1) is to define the Reynolds number in terms of known and relevant physical parameters of the nanorobot and its operating environment. The Reynolds number is a conventional index that provides a convenient measure of the turbulence or laminar flow characteristics of fluid flow around a moving nanorobot. If flow is expected to be laminar, the hydrodynamics of nanorobot motion is greatly simplified. For nanoscale dimensions in fluids of ordinary viscosities and velocities, *Re* is low and the flow is laminar [26]. The inertial force on the object is of order $F_{inertial} \cong \rho V^2 L^2$, and the viscous drag force is of order $F_{viscous} \cong \eta VL$. To keep moving forward, a nanorobot of size $L \cong 1$ micron and velocity $V \cong 10$ micron/sec. must apply $F_{inertial} \cong 10^{-4}$ f_N (femtonewtons $1fN = 10^{-15}$ N) and a much larger $F_{viscous} \cong 10$ fN of motive force [26]. For instance, if motive power to a swimming nanorobot with radius $R_{nano} = 1$ micron and velocity $V_{nano} = 1$ cm/sec. is suddenly stopped, then the nanorobot will "coast" to a halt in a time t_{coast} given in Ref. [4] by Eq. (2):

$$t_{coast} = \rho\left(R_{nano}\right)^2 / 15\eta = 0.1 \qquad (2)$$

where 0.1 is expressed in microsecond and in a distance $X_{coast} \cong V_{nano} t_{coast} = 1$ nm. Similarly, with v as the rotational frequency, if the nanorobot is rotating at a frequency $v_{nano} = 100$ Hz when its rotational power source is suddenly turned off, v_{nano} decays exponentially to zero in a time $t_{coast} \cong 0.1$ microsecond and stops after turning through an angle θ_{coast}, as expressed by Eq. (3):

$$\theta_{coast} = 2\pi v_{nano} \rho R_{nano^2} / 15\eta \qquad (3)$$

or 40 microradians in this instance [26].

It is anticipated that typical nanorobot motile forces and transit speeds through biological tissues of 1-100 pN and 0.1-1 mm/sec. [18b], respectively. The orthokinetic/perikinetic transition dimension is appropriate for the analysis of colloidal flocculation of nonmotile particles or even of low-energy density motile bacteria (~10^2 W/m^3 or 0.05 pW for an E. coli organism) employing 10^{-4} pW flagellar motors [38]. But in the case of high energy-density motile nanorobots (~10^9 W/m^3, up to ~1000 pW for a 1 micron device [18c]), Stokes law predicts a 1 micron spherical nanorobot must expend ~2 pW to traverse aqueous media at 1 cm/sec. [18d]. Propulsive efficiency for swimmers with spherical heads 10-40 times larger than their flagellar radius (optimum shape), using flagellar beats, ranges from 10% to 28% [12], raising the prospective nanorobot propulsive power input to 7-20 pW.

The virtual environment in this study is inhabited by nanorobots, biomolecules, obstacles and organ inlets (*Figure 1*). Each nanorobot measures 650 nm in length and 160 nm in diameter. The biomolecule has a diameter of ~10 nm, and each obstacle has a diameter of 120 nm. The organ inlets are 400 nm in height and width with inlet orifices 720 nm in diameter.

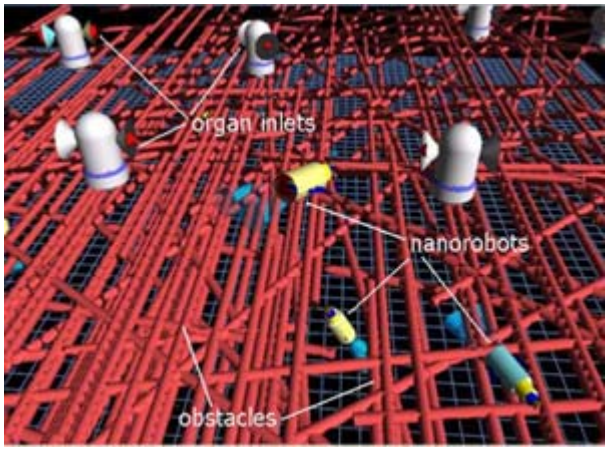

Figure 1. *Virtual environment, top camera view.*

The trajectories and positions of each molecule which must be captured and assembled were generated randomly; each one also has a probabilistic velocity and acceleration. In the implemented 3-D workspace, the simulations are velocity independent. Also, while some molecules have been captured (as seen in *Figure 2*), other molecules are manipulated and assembled internally by the robot arm inside the proposed nanorobot.

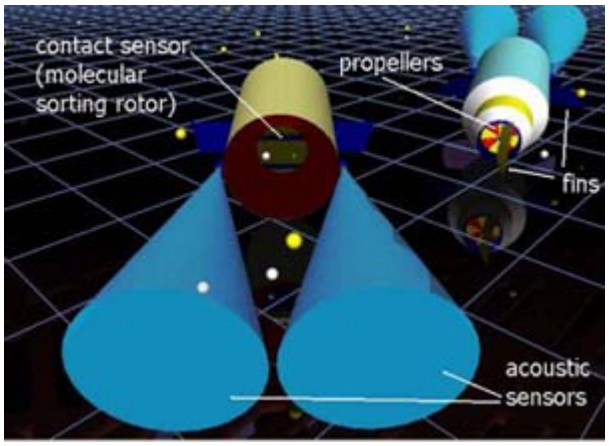

Figure 2. *Molecular identification.*

Nanorobot Design

Virtual reality was considered a suitable approach for nanorobot design and for the use of macro and microrobotics concepts given certain theoretical and practical aspects that focus on its domain of application. The nanodevice design must be robust enough to operate in an aqueous environment with movement having six degrees of freedom (see *Figure 1*).

The nanorobot design (*Figure 2*) is derived from biological models and is comprised of components such as molecular sorting rotors and a robot arm (telescoping manipulator) [15]. Different molecule types are distinguished by a series of chemotactic sensors whose binding sites have a different affinity for each kind of molecule [26]. The nanorobot exteriors considered in this design assume a diamondoid material to which may be attached an artificial glycocalyx surface that minimizes fibrinogen (and other blood protein) adsorption and bioactivity, thus ensuring sufficient biocompatibility for the nanorobot to avoid immune system attack [24]. Engineered nanorobots are not limited to behaviors extant in biology. The mechanics of artificial diapedesis, histonatation and ECM brachiation (tissue transit), intercellular passage, cytopenetration and in cyto locomotion by medical nanorobots have been explored elsewhere [18p], and a comprehensive discussion of nanorobotic biocompatibility, including mechanocompatibility during vascular surface transit, ECM transit, cytopenetration and intracellular navigation, has also appeared elsewhere [22a] along with specific pathways to avoid or suppress inflammation reactions [22b]. In special cases, such as the blood-brain barrier (BBB), the BBB ultrastructure has only been lightly studied, but occasional 0.5 micron perijunctional gaps (large enough to allow unfettered nanorobot passage) have been observed in frogs [18] and glycated albumin-gold colloid complexes injected into the mouse carotid yield “a few” gold particles in the perivascular neuropil after 15 min. [80]. This hints that the BBB might be sufficiently leaky to allow computer-controlled motile nanorobots to find and exploit preexisting openings to achieve noninflammatory artificial diapedesis through the BBB [22c]. Finally, phagocytosis and foreign-body granulomatous reaction are major issues for medical nanorobots intended to remain in the body for extended durations. An extensive discussion of nanorobotic phagocytosis [22d], including details of all steps in the phagocytic process and possible techniques for phagocyte avoidance and escape by medical nanorobots [22e], was published in 2003 [24].

Some concepts provided from underwater robotics [83] were assumed for nanorobot locomotion. The nanorobot kinematic response can be predicted using state equations, positional constraints, inverse kinematics and dynamics, while some individual directional component performance can be simulated using control system models of transient and steady-state response [7]. The nanorobots use a macrotransponder navigational system for the main aspects of the nanorobot positioning, which may allow high-positional accuracy in each nanorobot’s orientation [26]. Such a system might involve externally generated signals from beacons placed at fixed positions outside the skin [26,57]. Thus the delivery positions that represent organ inlets requiring proteins to be injected are located in well-known locations for the nanorobot. If these organ inlets are or are not scheduled for injection at time *t*, they change the team A (blue nanorobots) and team B (yellow nanorobots) delivery orifice colors in the simulation, opening or closing the orifice (*Figure 3*). This better enables visualization of the organ inlets in which the agents are performing their delivery in the current time step of the simulation. The assembled molecules are thus delivered to specific locations by nanorobots docking at 2 micron2 (~1.4 micron square) sites embedded at appropriate spatial intervals across the organ inlets’ orifice [25], which is open for the delivery. The assembled molecule can be pumped by the molecular sorting rotors in ~10 sec. [25].

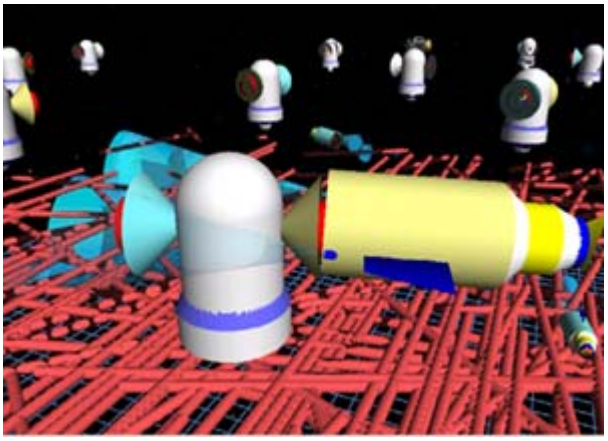

Figure 3. *Nanorobot molecule delivery.*

Note that we are dealing with nanorobots that are much larger than small individual molecules. Nanorobots must remain docked with adhesion energy of at least ~100 kT_{300} to avoid dislodgement due to molecular collisions with fluid molecules. Note that fluid shear stresses at arterial walls are 1-3 pN/micron^2 (arterial) [39]. Single integral proteins or ECM-attachment proteins require a dislodgement force ranging from ~1 pN to separate platelet surface-activated integrin GpIIb-IIIa from an attached fibrinogen molecule [77] up to ~100 pN for CD45 extraction from neutrophil membrane in ~10 sec [73]. Applying 30 pN of detachment force through a 10 nm extraction distance would expend the aforementioned ~100 kT300 (3 x 10-19 J), so a single-molecule protein attachment between nanorobot and dock would have a strength near the appropriate magnitude to withstand likely environment shear forces or Brownian motion collisions. A single nanorobot anchorage mechanism employing ~1,000 such attachment molecules per anchor would thus reduce the probability of nanorobot dislodgement effectively to zero [18e]. Microbiological examples of such secure anchorages abound, including the measured ~1,000 pN/micron^2 anchorage forces applied by individual fibroblasts during surface locomotion [37] and the 1,500 pN/micron^2 cell-cell adhesion between T cells and target cells [78]. The conservatively chosen 10 sec. residence time ensures completion of materials transfer. Change in affinity between docked and undocked states is computer controlled and may employ active mechanical clamps [18f] having little dependence on transition rates dictated by passive nanorobot surface-surface adhesivities.

The use of local perception should in most cases be quite sufficient for the overall set of tasks that the nanorobots are designed to perform. An explicit communication between each nanorobot partner sending the signal is required when a delivery is completed for the determined organ inlet, whereupon nanorobot B awaits a message from nanorobot A confirming that A has finished the delivery to the given organ inlet. Acoustic communication sensors [26] mounted within the nanorobot hull permit the nanorobot to communicate with its partner whether or not the organ inlet has received the required substance. In-vivo optical signaling may not be the practicable approach for communication [18m], though reliable detection of 1 Hz modulated heat signature signals from a 1,000 pW nanorobot at a range up to 100 microns may be feasible [18n]. Instead acoustic radiators very small in comparison to acoustic wavelength are point sources that produce a uniform intensity all angular directions. Formulas describing the behavior of such antennas are well known in acoustic science, for example, Massa's excellent summary in the 1972 "AIP Handbook" [52]. Receipt of nanorobot broadcasts at 10 MHz using a ~1 micron detector should have an

energy efficiency of ~5% [18g], taking into account the attenuation of acoustic waves traversing an aqueous medium [18h] and other factors. Assuming reasonable onboard nanorobot transmitter power levels, signals should be reliably received at interdevice separations up to 100-200 microns [18g]. Acoustic messaging over longer path lengths requires mobile signal amplifiers, dedicated fixed-position repeater stations, and other means [18i-18k]. By using the nanorobot's local perception as much as possible, and by sending the fewest possible messages to other nanorobots, unnecessary communication between the agents is reduced, thus minimizing energy consumption by the nanorobots. Nanorobots satisfy their energy requirements via the chemical combination of oxygen and glucose [26], both of which are plentiful in the human body.

The nanorobot includes external sensors [76] to inform it of collisions and to identify when it has encountered an obstacle that will require a new trajectory planning. Aspects of the nonstructured opaque surrounding workspace, like the interior of the human body where the nanorobot is acting, must be considered in the navigational sensing design. In robotics fields there are often many kind of sensors, such as infrared, computer vision, chemical sensors and so forth, that are normally used for robotics navigational purposes. Optical sensors have been widely applied in terrestrial mobile robotics, but these have an extremely limited range in a liquid environment. Some sensors, such as laser rangefinders [7], could be also used for underwater robotics but not for nanorobotics sensing because, for instance, the laser energy might excite or chemically alter the surrounding biomolecules that the nanorobot is trying to capture. Although the infrared sensor seems preferable for macroscale terrestrial robots, for underwater robots, the most common sensor approach involves the use of sonar systems. Similarly, the most addressable approach for nanorobots in nanomedicine is to use acoustic waves [26]. The blue cones shown in *Figure 2* represent regions that the robot's sonar can "hear." Scientific visualization techniques permit rapid and precise geometric analysis to simulate a sonar classification system [7].

Plane surfaces (three fins total) and bidirectional propellers are used for the navigation, which is comprised of two simultaneously counter-rotating screw drives for the propulsion [9]. Binary cues are being used to trigger the behavioral response as a common mechanism for action and for governing different phases of activity in tasks as done by social insects [13]. In this manner, activation of a motor behavior is not dependent on a specific perceptual cue, but rather on the decision that results from sensor processing. The information can be provided by either touch sensors or infra-red sensors. For example, a motor behavior created to make a robot rotate sin [Ω], where Ω assumes a set of possible predefined values, changes the robot route, avoiding a collision between the nanorobot and some undesirable obstacle. If the sensor is used then about the point of contact, it could specify when both sensors are in contact with some obstacle, as illustrated in *Figure 4*, and return a binary "11" value. The advantage is that the design of the motor behavior does not change when different sensor types or alternate feature extraction techniques are used because the information needed by the motor behavior is the same binary vector in both cases [44].

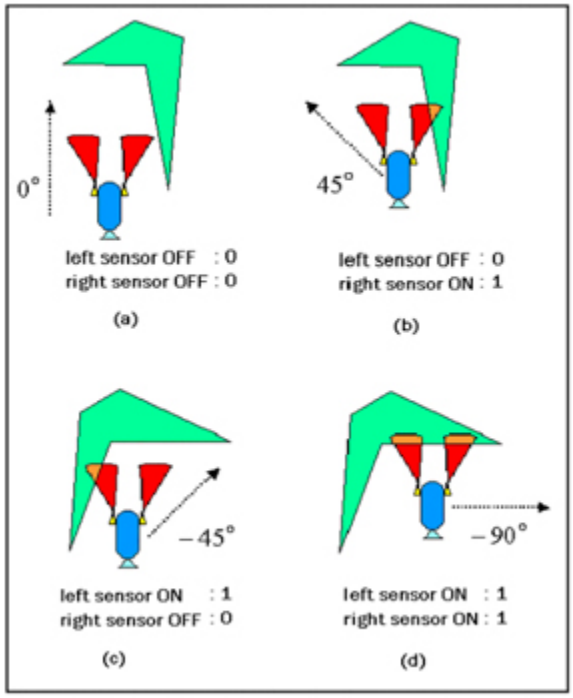

Figure 4. *Sensor-based navigational behavior.*

Evolutionary Decision

The authors intend to construct and demonstrate the applicability of multi-robot teams in timely sequenced work for capture, assembly, transport and delivery of biomolecular pieces to a predefined set of organ inlets. The use of multi-robot teams working cooperatively to achieve a single global task applied to nanotechnology is a field of research that is relatively new [9]. Research on collective robotics suggests that one should consider emulating the methods of the social insects [72] to build decentralized and distributed systems. Such systems are capable of accomplishing tasks through the interaction of agents with the same structures and preprogrammed actions and goals. Thus a careful decomposition of the main problem task into subtasks with action based on local sensor-based perception could generate multi-robot coherent behaviors [44].

The approach for the nanomedicine problem here could be described as two multi-robot teams that must cooperate interactively to feed a set of organ inlets in the virtual environment under study. The importance of cooperative teamwork has led us to choose a high-level decision control model with adaptive evolutionary characteristics. Note that the proposed nanorobot model here includes no kind of nanorobot self-replicating behavior [14]. Instead, our model uses an evolutionary approach strictly for the combinatorial analyses, allowing the nanorobots to react cooperatively in an uncertain environment with a well-defined preprogrammed set of actions. The model used here, often cited in the literature as genetic algorithms (GA), relies on concepts derived from evolution and genetics [10]. Each solution here is described as a chromosome regarding the nanorobot decision on how, when and what organ inlets to attend in the dynamic scenery. Each decision required to be taken by the nanorobot always follows the programmed set of actions rigidly pre-established in this design by the fitness/objective function. Equation (4) represents our fitness function, where the nanorobots maximize the protein levels for the selected organ inlets. The variable *y* induces the nanorobot to catch a number of molecules as closely as possible to the desired delivery mean, while *z* brings the nutritional levels as close as possible to .

$$Max\, f(r\Omega) = \sum_{t=1}^{n}\sum_{i=1}^{m} w_i^t - \left|y^t\right| - \left|z_i^t\right| \quad (4)$$

$$s.t.\ z_i^t = w_i^{t+1} - w_i^* \quad (5)$$

$$y^t = Q^t - d \quad (6)$$

$$Q^t = \sum x_i^t x_i^{\max} \quad (7)$$

$$x_i^t = \mu_i^t x_i^{\max} \quad (8)$$

$$\mu_i^t \le \Delta_i^{\max} \quad (9)$$

$$w_i^{t+1} = w_i^t - \gamma c_i^t + x_i^t \quad (10)$$

$$w_i^{\min} \le w_i^t \le w_i^{\max} \quad (11)$$

$$\mu_i^t \in \left\{\{0,100\} \vee \{0,1\}\right\} \quad (12)$$

$$\Omega \in \{A,B\} \quad (13)$$

where

r, t, i:	subscript denoting: robot, time, organ inlet.
w_i^*:	organ inlets' desirable nutritional target level.
y^t:	surplus/deficit to the desired assembled mean.
z:	keep the nutritional levels close to the target.
max, min:	upper and lower bound parameter.
A, B:	respective robotics teams.
n:	size of time in the simulated scenery.
m:	total of organ inlets to be fed.
L:	robot load capacity.
x_i^t:	substance amount injected in the organ inlet *i*.
Q^t:	total of assembled molecule by *r* in *t*.
w_i^t:	chemical state of the organ inlet *i* at time *t*.
c_i^t:	nutrients consumption by the organ inlet *i*.
d:	amount that r must assemble at period of t.
γ:	parameter to look ahead at nutritional levels.
μ_i^t:	Boolean variable.
Ω:	determines if *r* belongs to team *A* or *B*.
Δ:	maximum to be injected at organ *i* in *t*.

The chromosome representation comes from Eq. (12) and is taken in the following application:

rΩ: ←	1	0.3	1	0	0.5	0.2	…	0	1	0	0.8	1

where means: 0 is no delivery required for such organ inlet; 1 is to inject the full amount pre-established to that organ inlet; otherwise, it means to inject some specific percentage from the amount of permitted injection at time *t*. We have decomposed the total set of organ inlets, assigning for each pair of nanorobots a specified number of organ inlets to be attended by the nanorobots at each time step of the simulation. Each pair is comprised of nanorobots from team *A* and *B*. The organ inlets selected to be fed at time *t* have to be fed first by the agent *A*, then by *B* and so forth. Both agents must take care to avoid applying an overdose or deficiency of the injected substances. The multi-robot team behavior interaction rule is described in *Table 1*, with $\Omega \in \{A,B\}$, Ω denoting if the robot *r* belongs to team *A* or *B*; min is the minimum defined to be captured by each robot at time step *t*, where *e,g* and *h* represent the kind of molecule to be assembled by *r*, therefore:

$$\beta \begin{cases} \Omega \equiv A \Rightarrow \beta = e, \\ \Omega \equiv B \Rightarrow \beta = h \end{cases} \quad (14)$$

$$\delta = g \quad (15)$$

Step 1: r_Ω walk randomly to capture and ;
Step 2: if $\sum$ = $\sum$ → assemble $f(r_\Omega)$= + ;
Step 3: if $\sum f(r_\Omega) <$ min repeat step 1;
Step 4: r_Ω achieve next delivery goal regarding the delivery queue;
Step 5: if delivery_Orifice_is_Open = true → next step; otherwise: go to step 9;
Step 6: if delivery_Permission = true → next step; otherwise: go to step 9;
Step 7: if NOT_overdose = true → next step; otherwise: go to step 9;
Step 8: delivery: $f(r_\Omega) = f(r_\Omega) - 1$;
Step 9: if $f(r_\Omega) > 0$ → repeat step 4;
Step 10: r_Ω → complete the verification route;
Step 11: repeat step 1;

Table 1. *Collective nanorobotics teams interaction rule.*

The real-time [46,58] and parallel processing techniques [84] were used, where both teams react adaptively to any stimulus produced by their partners' decisions, with the model visualization in real time. The study of smart multi-robot behavior in a single global environment enables concepts related to the use of local perception for reactive agents [5,44]. Multidisciplinary control design [11] addresses the nanorobot's multi-modular system architecture (*Figure 5*). A feedforward neural networks model discussed below was used for the nanorobot motion control, wherein each nanorobot visits in a shorter time the organ inlets that were pre-attributed to that nanorobot to gather information for the next-time step decision from the 3-D workspace (*Figure 6*).

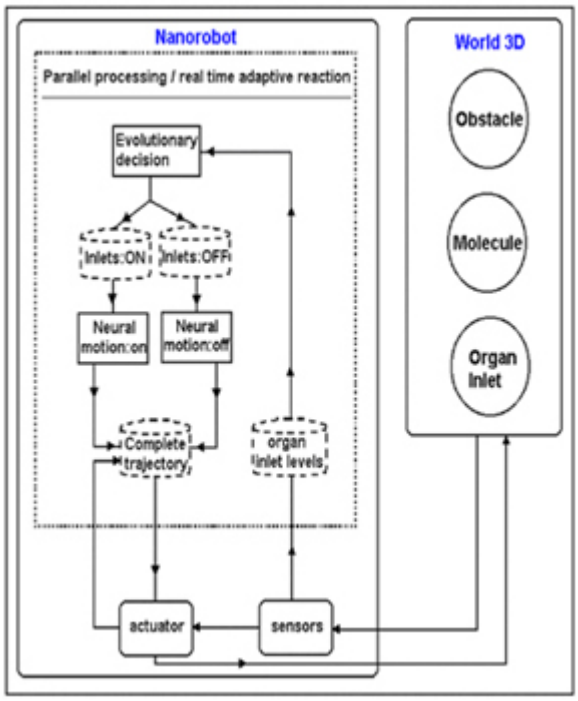

Figure 5. *Multimodular system architecture.*

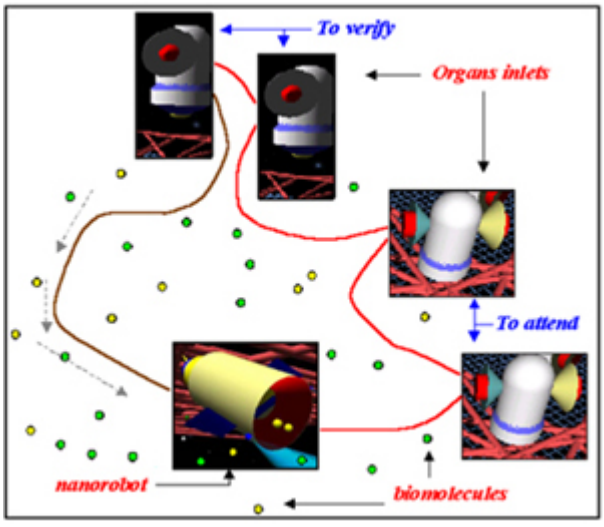

Figure 6. *Nanorobot gathers information and biomolecules.*

Neural Motion

A connectionist model using artificial neural networks was chosen for the motion control and shortest-path problem solution, beginning with a dynamic combinatorial problem for each time-step simulation. The classical problem of finding an optimal three-dimensional shortest path avoiding 3-D polygonal obstacles is typically NP-hard [3]. The use of a nondeterministic approach to solve the motion control seems to be the appropriate technique in such cases [30]. A feedforward or acyclic network was implemented because of its

suitability for probabilistic calculations. The particular model implemented here is a stochastic feedforward neural network [34], which requires a lower computational effort in comparison with a backpropagation algorithm [32] and a better performance in comparison with a greedy heuristic approach [81]. The features of the algorithm for the implemented neural network could be represented by Eq. (16):

$$pa\left(X_j\right) \subseteq \left\{X_1,\ldots,X_{j-1}\right\} \tag{16}$$

where *X* represents a vector, consisting of the two-valued random variables *X1, X2,…, Xn,* defining a topology composed of *N* stochastic neurons. With *n* representing the range of hidden layers, which leads the network to be optimized at the time step *t*, it represents each destiny to be achieved for $r\Omega$ throughout the simulation. The units in the network are organized into a two-dimensional matrix S_{mn}, with *n* rows by *m* columns, where *n* and *m* are the costs matrix of destinations for each evolutionary agent, which tries to complete its set of tasks successfully as fast as possible. Let the output of the unit in row *i* and column *j* be $p_{ij} = 1$, where $i \neq j$. This means that the referred destination is visited at the i^{th} stop, with $p_{ij} = 0$ otherwise. Therefore, a solution cost for each agent routing could be expressed by Eq. (17).

$$Min \quad P_r^t = \sum_{i=1}^{m}\sum_{j=1}^{n} p_{ij}s_{ij} \tag{17}$$

s.t.

$$p_{ij} = 1 \Leftarrow i \equiv pa\left(X_{j-1}\right) \wedge j \equiv pa\left(X_j\right) \tag{18}$$

$$p_{ij} = 0 \Leftarrow c.c. \tag{19}$$

The routes are comprised, respectively, of the organ inlets to be supplied and the organ inlet whose nutritional level is to be verified, represented by route on and route off. The nanorobot performs the trajectory visiting the subset of organ inlets assigned to it, first executing the whole delivery route and afterwards beginning the verification route. *Figure 7* shows an illustrative representation of the trajectories process that receives from the neural motion control module to improve their performance.

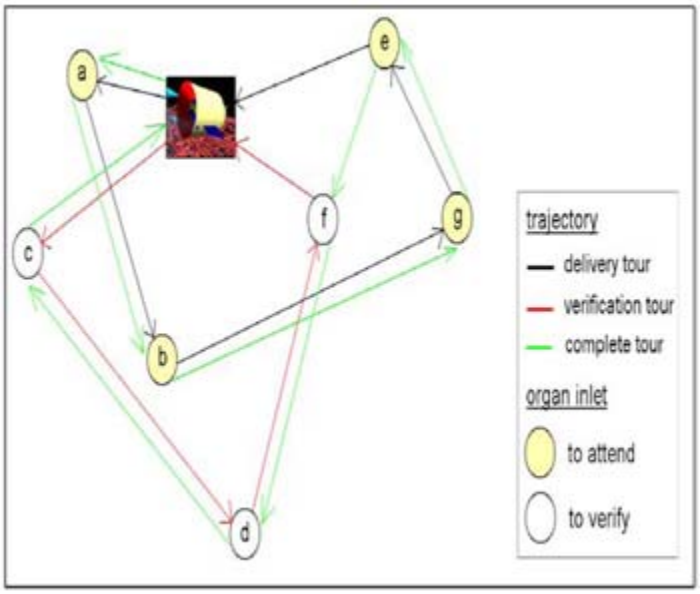

Figure 7. *Complete trajectory comprised by delivery and verification tour.*

One positive aspect of a feedforward neural network (see *Table 2*) is that it requires low computational effort to achieve motion control in a workspace with six degrees of freedom [32]. The obstacles are located in probabilistic positions (*Figure 8* and *9*).

```
timeControl=Φ;
time_begin = time(NULL);
do
{//Generate Feedforward ANN Solutions
 j=0;
 for(move=0;move<nDestiny;move++)
 {  neuronActive=randomLayer(nDestiny-move);
    // Take the activated neurons.
    search.sequence[j]=neuronSelect[neuronActive];
    for(i=neuronActive;i<(nDestiny-move)-1;i++)
    {  neuronSelect[i]=neuronSelect[i+1];
    }
    j++;
 }
 // Compare the actual cost and take this
 // solution if it has the best cost.
 reckonNeuralCost();
 time_end = time(NULL);
}while(time_end - time_begin < timeControl);
```

Table 2. *Feedforward ANN pseudo code.*

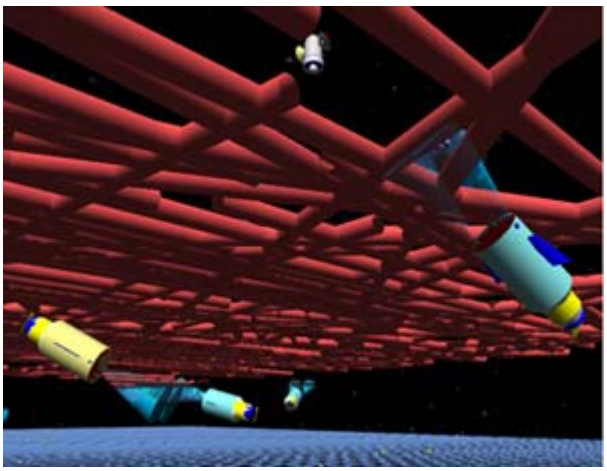

Figure 8. *Sensing obstacles.*

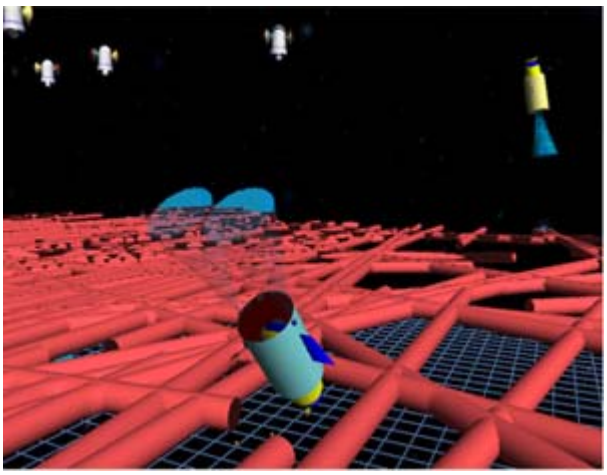

Figure 9. *Nanorobot obstacle avoidance.*

Conclusion

Biomolecular machine system designs that are capable of successfully accomplishing a set of pre-programmed tasks in a 3-D workspace are a new challenge for control investigation. This article described the study of an automation model and the respective visualization tools to follow up the analyses for the control theory development based on experimental results.

The nanorobot has required a decision control that demonstrates the most effective methodology for stochastic surroundings when only a low-level action description does not attend a large number of complex circumstances in a dynamic environment. A coherent team behavior was suitably achieved demonstrating satisfactory performance in controlling the organ inlets' nutritional levels. For the delivery mean was established an amount of 300 proteins as a relative symbolic amount to set up a target, which has to be managed by our nanorobots through the genetic algorithm. In the simulation such amount was successfully attended as observed in *Table 3*. As an exemplar target, the nutritional level value of 50% of the relative organ inlet nutritional capacity was adopted. Levels lower than 20% or higher than 80%

are then characterized as a possible deficiency or as an overdose case. In the simulations (*Figure 10*), no occurrences of nutritional levels beyond desired ranges were observed, illustrating successful collective nanorobot coherent behavior.

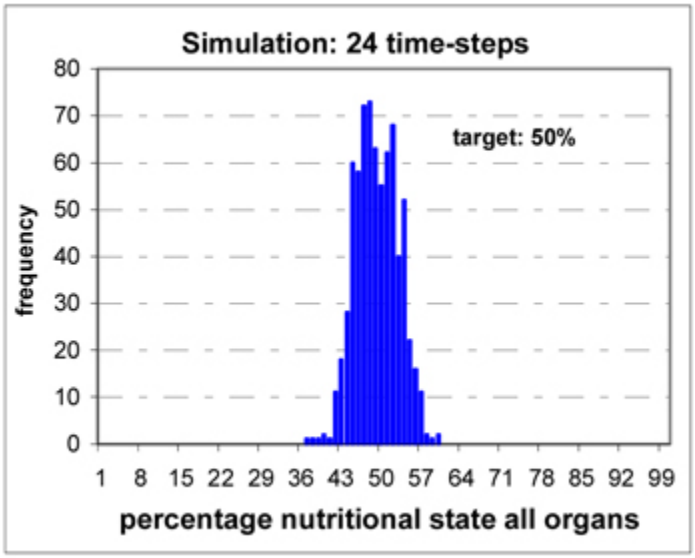

Figure 10. *Histogram with nutritional levels behaviors.*

Time	1	2	3	4	5	6	7	8	9	10	11	12	13	14	15	16	17	18	19	20	21	22	23	24
Delivery target	300	300	300	300	300	300	300	300	300	300	300	300	300	300	300	300	300	300	300	300	300	300	300	300
Lowest level	45	44	41	45	43	43	43	46	42	42	39	42	40	42	37	38	42	43	43	43	40	43	45	43
Highest level	54	57	55	57	56	55	57	55	58	56	58	57	60	57	56	57	56	59	57	60	55	57	56	56

Table 3. *GA results: the attended delivery target, highest and lowest levels.*

The nanorobot has required a motion control model having one or two main aspects: dynamic optimization of the trajectory distances to enable the delivery of assembled biomolecules and real-time analyses for a required trajectory with avoidance of obstacles. The neural motion control was successfully used with real-time response for the circumstance where the nanorobots must capture molecules and visit a predefined set of delivery points. Such technique has also permitted avoiding random obstacles and collision with other mobile nanorobots, and minimized the time required. As we may observe, these tasks were satisfactorily accomplished using the neural networks approach. The nanorobots calculated their complete trajectories with a cost minimization of ~37% in the required distance (*Figure 11*), which shows good improvement in comparison with a greedy solution for the motion control optimization.

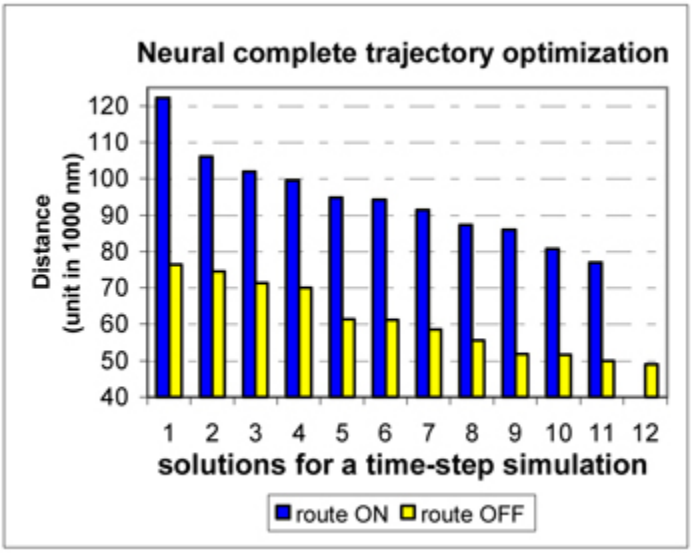

Figure 11. *Motion control cost minimization.*

The presented work has considered the importance of nanosystems design using a modular architecture comprised of an evolutionary decision model and a sensor-based neural motion system as a feasible approach for the development of smart mobile nanorobots, applied in this instance to nanomedicine. Important aspects related to nanomanipulation that must be incorporated in a control simulator intended to represent a 3-D environment at the nanoscale was described. The model addressed in this work might be a promising system design for the investigation of positional assembly automation in nanotechnology.

Realizing revolutionary applications of nanorobots to health or environmental issues raises new control challenges. The design and the development of complex nanosystems with high performance should be addressed via simulation to help pave the way for future medical nanorobotic systems.

Acknowledgments

The authors thank Tad Hogg for helpful comments on an earlier version of this article.

References

[1] Adleman, L.M. **"On Constructing A Molecular Computer."** *DNA Based Computers*, 1995.

[2] Bachand, G.D. and Montemagno, C.D. "Constructing Organic/Inorganic NEMS Devices Powered by Biomolecular Motors." *Biomedical Microdevices* (v2, 2000), pp179-184.

[3] Baraff, D. "Dynamic Simulation of Non-Penetrating Rigid Bodies." PhD thesis, Dept. of Computer Science, Cornell Univ., Ithaca, N.Y, 1992.

[4] Berg, H.C. "Dynamic Properties of Bacterial Flagellar Motors." *Nature* (v249, May 1974), pp77-79.

[5] Bojinov, H.; Casal, A.; and Hogg, T. "Multiagent Control of Modular Self-Reconfigurable Robots." *Artificial Intelligence* (v142, 2002), pp99-120.

[6] Brooks, R. "Artificial Life and Real Robots." MIT Press, 1992.

[7] Brutzman, D.P.; Kanayama, Y.; and Zyda, M.J. "Integrated Simulation

for Rapid Development of Autonomous Underwater Vehicles." IEEE Autonomous Underwater Vehicle Conf., IEEE Oceanic Engg. Society, Washington, D.C., June 1992, pp3-10.

[8] Casal, A.; Hogg, T.; and Cavalcanti, A. "Nanorobots as Cellular Assistants in Inflammatory Responses." IEEE BCATS Biomedical Computation at Stanford 2003 Symp., IEEE Computer Society, Stanford, Calif., Oct. 2003.

[9] Cavalcanti, A. and Freitas, R.A. Jr. **"Nanorobotics Control Design: A Collective Behavior Approach for Medicine."** IEEE *Trans.* on Nanobioscience (v4, n2), pp133-140.

[10] Cavalcanti, A. **"Assembly Automation with Evolutionary Nanorobots and Sensor-Based Control Applied to Nanomedicine."** IEEE *Trans.* on Nanotechnology (v2, n2, June 2003), pp82-87.

[11] Chen, W. and Lewis, K. "A Robust Design Approach for Achieving Flexibility in Multidisciplinary Design." *AIAA Journal* (v37, n8, 1999), pp982-990.

[12] Chwang, A.T. and Wu, T.Y. "A Note on the Helical Movement of Micro-Organisms." *Proc.* of Roy. Soc. Ser. B (v178, 1971), pp327-346.

[13] Downing, H.A. and Jeanne, R.L. "Nest Construction by the Paperwasp, Plistes: A Test of Stigmergy Theory." *Animal Behavior* (v36, 1988), pp1729-1739.

[14] Drexler, K.E.; Forrest, D.; Freitas, R.A. Jr.; Hall, J.S.; Jacobstein, N.; McKendree, T.; Merkle, R.; and Peterson, C. **"A Debate about Assemblers."** Institute for Molecular Mfg., 2001.

[15] Drexler, K.E. "Nanosystems: Molecular Machinery, Manufacturing, and Computation." John Wiley & Sons, 1992.

[16] Drucker, H.D.; Wu, D.; and Vapnik, V. "Support Vector Machines for Spam Categorization." IEEE *Trans.* on Neural Networks (v10, n5), pp1048-1054.

[17] Fishbine, G. "The Investor's Guide to Nanotechnology & Micromachines." John Wiley & Sons, 2001.

[18] Fraser, P.A. and Dallas, A.D. "Permeability of Disrupted Cerebral Microvessels in the Frog." J. Physiol. (v461, 1993), pp619-632.

[19] Freitas, R.A. Jr. and Merkle, R.C. "A Minimal Toolset for Positional Diamond Mechanosynthesis." *Journal of Comput. Theor. Nanosci.* (2005). Submitted.

[20] Freitas, R.A. Jr. "Progress in Nanomedicine and Medical Nanorobotics." Rieth, M. and Schommers, W. eds. *Handbook of Theoretical and Computational Nanotechnology*. Stevenson Ranch, Calif.: American Scientific Publishers, Oct. 2005. In press.

[21] Freitas, R.A. Jr., **"Current Status of Nanomedicine and Medical Nanorobotics."** (Invited Survey) - J. Comput. Theor. Nanosci. 2 (March 2005):1-25.

[22] Freitas, R.A. Jr. **"A Simple Tool for Positional Diamond Mechanosynthesis, and Its Method of Manufacture."** U.S. Provisional Patent Application No. 60/543,802, filed Feb. 11, 2004; U.S. Patent Pending, Feb. 11, 2005.

[23] Freitas, R.A. Jr. and Merkle, R.C. **"Kinematic Self-Replicating Machines."** Georgetown, Texas: Landes Bioscience, 2004.

[24] Freitas, R.A. Jr., **"Nanomedicine, Volume IIA: Biocompatibility."** Georgetown, Texas: Landes Bioscience, 2003, Sections (a) 15.5, (b) 15.2.4, (c) 15.3.6.5, (d) 15.4 and (e) 15.4.3.6.

[25] Freitas, R.A. Jr. and Phoenix, C.J. **"Vasculoid: A Personal Nanomedical Appliance to Replace Human Blood." J. Evol. Technol., 11, 2002.**

[26] Freitas, R.A. Jr. **"Nanomedicine, Vol. I: Basic Capabilities."** Georgetown, Texas: Landes Bioscience, 1999, Sections (a) 9.4, (b) 9.4.4.2, (c) 6.5.3, (d) 9.4.2.4, (e) 9.4.3.3, (f) 5.4.1, (g) 7.2.2, (h) 4.9.1.3, (i) 6.4.1, (j) 7.3, (k) 8.3.5, (m) 4.9.4, (n) 7.2.3 and (p) 9.4.4.

[27] Fukuda, T. and Arai, T. "Prototyping Design and Automation of Micro/Nano Manipulation System." *Proc.* of IEEE Int'l Conf. on Robotics and Automation (ICRA, 2000), pp192-197.

[28] Geppert, L. "The Amazing Vanishing Transistor Act." *IEEE Spectrum Magazine*, Oct. 2002, pp28-33.

[29] Grefenstette, J.J. and Schultz, A. "An Evolutionary Approach to Learning in Robots." **Machine Learning Workshop on Robot Learning**. New Brunswick, N.J., 1994.

[30] Grzeszczuk, R.; Terzopoulos, D.; and Hinton, G. "NeuroAnimator: Fast Neural Network Emulation and Control of Physics-Based Models." Cohen, M. ed., *Proc.* of ACM SIGGRAPH 1998 Conf., pp142-148.

[31] Guthold, M. "Controlled Manipulation of Molecular Samples with the Nano-Manipulator." IEEE/ASME *Trans.* on Mechatronics (v5, n2, 2000), pp189-198.

[32] Hagan, M.T.; Demuth, H.B.; and Jesús, O.D. "An Introduction to the Use of Neural Networks in Control Systems." *Int'l Journal of Robust and Nonlinear Control*. John Wiley & Sons (v12, n11, Sept. 2002), pp959-985.

[33] Hagiya, M. "From Molecular Computing to Molecular Programming." *Proc.* of 6th DIMACS Workshop on DNA Based Computers, Leiden, Netherlands, 2000, pp198-204.

[34] Haykin, S. "Neural Networks A Comprehensive Foundation." 2nd ed., N,J.: Prentice Hall, 1999.

[35] Hellemans, A. "German Team Creates New Type of Transistor-Like Device." *IEEE Spectrum Magazine*, Jan. 2003, pp20-21.

[36] Helmer, G.; Wong, J.S.K.; Honavar, V.; and Miller, L. "Intelligent Agents for Intrusion Detection." *Proc.* of IEEE Information Technology Conf., Syracuse, N.Y., Sept. 1998, pp121-124.

[37] James, D.W. and Taylor, J.F. "The Stress Developed by Sheets of Chick Fibroblasts in Vitro." Exp. Cell Res. (v54, 1969), pp107-110.

[38] Jones, C.J. and Aizawa, S.-I. "The Bacterial Flagellum and Flagellar Motor: Structure, Assembly and Function." Adv. Microbial Physiol. (v32, 1991), pp109-172.

[39] Kamiya, A.; Bukhari, R.; and Togawa, T. "Adaptive Regulation of Wall Shear Stress Optimizing Vascular Tree Function." *Bull. Math. Biol.* (v46, 1984), pp127-137.

[40] Katz, E.; Riklin, A.; Heleg-Shabtai, V.; Willner, I.; and Bückmann, A.F."Glucose Oxidase Electrodes Via Reconstitution of the Apo-Enzyme: Tailoring of Novel Glucose Biosensors." *Anal. Chim. Acta.* (v385, 1999), pp45-58.

[41] Khatib, M.; Bouilly, B.; Simeon, T.; and Chatila, R. "Indoor Navigation with Uncertainty Using Sensor Based Motions." *Proc.* of 1997 IEEE Int'l Conf. on Robotics and Automation, Albuquerque, N.M., 1997, pp3379-3384.

[42] Kretly, L.C.; Almeida, A.F.L.; Oliveira, R.S.; Sasaki, J.M.; and Sombra, A.S. "Electrical and Optical Properties of CaCu3 Ti4 O12 (CCTO) Substrates for Microwave Devices and Antennas." *Microwave and Optical Technology Letters* (New York: EUA, v39, n2, Oct. 2003), pp145-150.

[43] Krishnamurthy, B. and Rosemblum, D.S. "Yeast: A General Purpose Event-Action System." IEEE *Trans.* on Software Engg. (v21, n10, Oct. 1995), pp845-857.

[44] Kube, C.R. and Zhang, H. “Task Modelling in Collective Robotics.” *Autonomous Robots* (v4, n1, 1997), pp53-72.

[45] Kumar, M.N.V.R. “Nano and Microparticles as Controlled Drug Delivery Devices.” *Journal of Pharmacy Parmaceutical Science* (v3, n2, 2000), pp234-258.

[46] Lehoczky, J.; Sha, L.; and Ding, Y. “The Rate Monotonic Scheduling Algorithm.” Santa Monica, Calif.: IEEE Computer Society Press, Dec. 1989, pp166-171.

[47] Lewis, M.A. and Bekey, G.A. “The Behavioral Self-Organization of Nanorobots Using Local Rules.” *Proc.* of IEEE Int’l Conf. on Intelligent Robots and Systems, Raleigh, N.C., 1992.

[48] Lyons, K. and Wang, Y. “An Open Architecture for Virtual Reality in Nano-Scale Manipulation, Measurement and Manufacturing (M3).” 8th Foresight Conf. on Molecular Nanotechnology, 2000.

[49] MacNeil, J.S. **“Nanorobot Pioneer Reveal Status of Simulator, Stem Cell Work.”** *NanoBiotech News* (v2, n36, Sept. 2004), pp4-5.

[50] Makaliwe, J.H. and Requicha, A.A.G. “Automatic Planning of Nanoparticle Assembly Tasks.” *Proc.* of IEEE Int'l Symp. on Assembly and Task Planning, Fukuoka, Japan, 2001, pp288-293.

[51] Martel, S.; Madden, P.; Sosnowski, L.; Hunter, I.; and Lafontaine, S.”NanoWalker: A Fully Autonomous Highly Integrated Miniature Robot for Nano-Scale Measurements.” *Proc.* of European Optical Society and SPIE Int’l Symp. on Envirosense, Microsystems Metrology and Inspection (v3825, Munich, Germany, 1999), pp64-76.

[52] Massa, F. “Chapter 3i. Radiation of Sound.” Gray, D.E. ed., *American Institute of Physics Handbook*. 3rd ed., New York: McGraw-Hill, 1972, pp3.139-3.153.

[53] Matellan, V.; Fernandez, C.; and Molina, J.M. “Genetic Learning of Fuzzy Reactive Controllers.” *Robotics and Autonomous Systems* (v225, n2, 1998), pp33-41.

[54] McDevitt, M.R.; Ma, D.; Lai, L.T.; Simon, J.; Borchardt, P.; Frank, R.K.;Wu, K.; Pellegrini, V.; Curcio, M.J.; Miederer, M.; Bander, N.H.; and Scheinberg, D.A. **“Tumor Therapy with Targeted Atomic Nanogenerators.”** *Science* (v294, Nov. 16, 2001), pp1537-1540.

[55] Menezes, A.J.; Kapoor, V.J.; Goel, V.K.; Cameron, B.D.; and Lu, J.-Y. “Within a Nanometer of Your Life.” *Mechanical Engineering* (v123, n8, Aug. 2001), pp54-58.

[56] Merkle, R.C. and Freitas, R.A. Jr. “Theoretical Analysis of a Carbon-Carbon Dimer Placement Tool for Diamond Mechanosynthesis.” *Journal of Nanoscience and Nanotechnology* (Aug. 3, 2003), pp319-324.

[57] Merkle, R.C. “Nanotechnology and Medicine.” *Advances in AntiAging Medicine* Mary Ann Liebert Press, 1996, pp277-286.

[58] Mok, A. and Chen, D. “A Multiframe Model for Real-Time Tasks.” IEEE *Trans.* on Software Engg. (v23, n10, 1997), pp635-645.

[59] Mokhoff, N. **“Education Overhaul Urged for Nanotech Revolution.”** *EE Times, Feb. 2003.*

[60] Moore, S.K. “Just One Word – Plastics.” Special R&D Report, Organic Electronics, *Spectrum*, Sept. 2002, pp55-59.

[61] **National Science Foundation**.

[62] Okamoto, T. and Ishida, Y. “A Performance Analysis of a Mobile Anti-virus System." *Proc.* of AROB 02, 2002, pp132-135.

[63] Peng, J.; Freitas, R.A. Jr.; Merkle, R.C.; Ehr, J.R.V.; Randall, J.N.; and Skidmore, G.D. “Theoretical Analysis of Diamond Mechanosynthesis. Part III. Positional C2 Deposition on Diamond C(110) Surface using Si/Ge/Sn-Based Dimer Placement Tools.” Journal of Comput. Theor.

Nanosci. (2005). Submitted.

[64] Peng, J.; Freitas, R.A. Jr.; and Merkle, R.C. “Theoretical Analysis of Diamond Mechanosynthesis. Part I. Stability of C2 Mediated Growth of Nanocrystalline Diamond C(110) Surface.” *Journal of Comput. Theor. Nanosci.* (v1, March 2004), pp62-70.

[65] Petrie, C.J. **Agent-Based Engineering, the Web, and Intelligence**. *IEEE Expert*, Dec. 1996.

[66] Ramia, M.; Tullock, D.L.; and Thien, N.P. “The Role of Hydrodynamic Interaction in the Locomotion of Microorganisms.” *Biophysics Journal* (v65, 1993), pp755-778.

[67] Reppesgaard, L. “Nanobiotechnologie: Die Feinmechaniker der Zukunft nutzen Biomaterial als Werkstoff.” *Computer Zeitung* (v36, Sept. 2, 2002), p22.

[68] Requicha, A.A.G. “Nanorobots, NEMS and Nanoassembly.” IEEE ICRA Int'l Conf. on Robotics and Automation, special issue on Nanoelectronics and Nanoprocessing, Taipei, Taiwan (v91, n11, Nov. 2003), pp1922-1933.

[69] Requicha, A.A.G.; Resch, R.; Montoya, N.; Koel, B.E.; Madhukar, A.; and Will, P. “Toward Hierarchical Nanoassembly.” IEEE/RSJ Int'l Conf. on Intelligent Robots & Systems, Kyongju, Korea, 1999.

[70] Rietman, E.A. “Molecular Engineering of Nanosystems. Biological Physics Series.” New York: Springer-Verlag, 2001.

[71] Roco, M.C. **Government Nanotechnology Funding: An International Outlook.”** National Science Foundation, June 2003.

[72] Seely, T.D.; Camazine, S.; and Sneyd, J. “Collective Decision-Making in Honey Bees: How Colonies Choose Among Nectar Sources.” *Behavioral Ecology and Sociobiology* (v28, 1991), pp277-290.

[73] Shao, J.Y. and Hochmuth, R.M. “Mechanical Anchoring Strength of L-Selectin, Beta2-Integrins, and CD45 to Neutrophil Cytoskeleton and Membrane.” *Biophys. J.* (v77, 1999), pp587-596.

[74] Sitti, M. and Hashimoto, K. “Teleoperated Nano Scale Object Manipulation.” *Recent Advances on Mechatronics*. Springer Verlag, Kaynak, O., ed., 1999, pp172-178.

[75] Stracke, R.; Böhm, K.J.; Burgold, J.; Schacht, H.; and Unger, E. “Physical and Technical Parameters Determining the Functioning of a Kinesin-Based Cell-Free Motor System.” *Nanotechnology* (v11, 2000), pp52-56.

[76] Sun, J.; Gao, M.; and Feldmann, J. “Electric Field Directed Layer-by-Layer Assembly of Highly Fluorescent CdTe Nanoparticles.” *Journal of Nanoscience and Nanotechnology*. American Scientific Publishers (v1, n2, 2001), pp21-27.

[77] Sung, K.-L.P.; Frojmovic, M.M.; O’Toole, T.E.; Zhu, C.; Ginsberg, M.H.; and Chien, S. “Determination of Adhesion Force Between Single Cell Pairs Generated by Activated GpIIb-IIIa Receptors.” *Blood* (v81, 1993), pp419-423.

[78] Sung, K.-L. P.; Sung, L.A.; Crimmins, M.; Burakoff, S.J.; and Chien, S. “Determination of Junction Avidity of Cytolytic T Cell and Target Cell.” *Science* (v234, 1986), pp1405-1408.

[79] Toth-Fejel, T. “Agents, Assemblers, and ANTS: Scheduling Assembly with Market and Biological Software Mechanisms.” *Nanotechnology* (v11, 2000), pp133-137.

[80] Vorbrodt, A.W. and Dobrogowska, D.H. “Interaction of Glycated Albumin-Gold Complexes with Mouse Brain Microvascular Endothelium.” Folia Histochem. Cytobiol. (v37, 1999), pp3-10.

[81] Voss, S. “Meta-Heuristics: Advances and Trends in Local Search

Paradigms for Optimization." Meta-Heuristics Int'l Conf., Kluwer, 1998.

[82] Wieland III, C.F. et al., **"Is the US Nanotechnology Investiment Paying Off?"** Intellectual Property, *Small Times* Magazine, Jan./Feb. 2004.

[83] Whitcomb, L.L. "Underwater Robotics: Out of the Research Laboratory and Into the Field." IEEE Int'l Conf. on Robotics and Automation, San Francisco, 2000, pp85-90.

[84] Wurll, C.; Henrich, D.; and Wörn, H. "Parallel On-Line Motion Planning for Industrial Robots." 3rd ASCE Specialty Conf. on Robotics for Challenging Environments (Robotics 1998), New Mexico, pp308-314.